

Electronic properties of chelating dicarbene palladium complexes: A combined electrochemical, NMR and XPS investigation

Gabriella Buscemi^a, Marino Basato^{a,b}, Andrea Biffis^a, Armando Gennaro^a, Abdirisak Ahmed Isse^{a,*}, Marta Maria Natile^b, Cristina Tubaro^{a,*}

^a Dipartimento di Scienze Chimiche, Università di Padova, via Marzolo 1, I-35131 Padova, Italy

^b ISTM – CNR and INSTM, Dipartimento di Scienze Chimiche, Università di Padova, via Marzolo 1, I-35131 Padova, Italy

ARTICLE INFO

Article history:

Received 23 March 2010
Received in revised form
21 June 2010
Accepted 22 June 2010
Available online 30 June 2010

Keywords:

N-heterocyclic dicarbene ligands
Palladium dicarbene complexes
Cyclic voltammetry of complexes
XPS of palladium
NMR of dicarbene complexes

ABSTRACT

A series of N-heterocyclic dicarbene palladium(II) complexes has been characterised combining different techniques (cyclic voltammetry, XPS and ¹³C NMR spectroscopy), in order to evaluate the influence of the dicarbene ligand on the electronic properties of the metal centre. The data obtained with the three techniques give relevant information, cyclic voltammetry appearing the most useful approach. In addition, the observed variations of the physico-chemical properties of the complexes confirm the possibility of finely tuning the electronic properties of the palladium(II) centre by changing the characteristics of the dicarbene ligand (wingtip substituents, bridging group between the carbene units, type of heterocyclic ring).

© 2010 Elsevier B.V. All rights reserved.

1. Introduction

A crucial factor for the development and optimization of transition metal complex catalysts is the control of both steric and electronic properties at the metal centre, aimed at rationally tailoring the catalyst to the peculiar reaction and substrates under study. Consequently, the development of methods for a precise description and quantification of these properties is essential and has been actively pursued [1].

We have been interested for some time in the use of chelating di-N-heterocyclic carbene (NHC) palladium(II) complexes (Chart 1) as catalysts for the hydroarylation of alkynes with simple arenes [2]. In the proposed catalytic cycle for this reaction, highly electrophilic species of palladium(II) are involved [3,4]; consequently, it may be reasonably assumed that the electronic density at the metal centre has an important influence on the efficiency of the catalyst. As a matter of fact, we have previously shown through kinetic studies that the catalytic activity of the illustrated palladium dicarbene complexes depends on the chemical nature of the NHC ligands [2].

Several spectroscopic and electrochemical studies have been previously performed to determine the electron-donating properties of mono-NHC ligands [5–7]. In this paper, we have extended these investigations to chelating NHC palladium(II) complexes by combining different techniques, namely cyclic voltammetry, XPS and ¹³C NMR spectroscopy. The first of these techniques allows the determination of the redox potentials of the carbene complexes and, in particular, of the Pd(II)/Pd(0) reduction potential, which can be a useful probe for the electron density at the metal. Low reduction potentials are indeed expected when the ligands coordinated to the metal are strongly electron-donating. For example, Demonceau and co-workers [6] have determined the redox potentials, E^\ominus , of NHC-Ru^{II} complexes, showing the existence of a correlation between the E^\ominus and the catalytic activity in atom transfer radical polymerisation (ATRP). XPS analysis of the 3d and 3p levels in palladium(II) complexes is also a powerful tool to evaluate the ligand donor ability, thanks to the strict relation between the electron bonding energies and the electron density on the metal centre [8]. Finally, further information on the donor strength of an NHC ligand can be gained by the analysis of the ¹³C NMR spectra of the coordinated carbene carbon, as recently demonstrated by Huynh et al. [9]. All these techniques have been applied to the dibromo palladium complexes **1–5** (Chart 1) and, in part, to their dicationic partners obtained by halogen removal *via* silver ions.

* Corresponding authors. Fax: +39 049 8275223.

E-mail addresses: abdirisak.ahmedisse@unipd.it (A.A. Isse), cristina.tubaro@unipd.it (C. Tubaro).

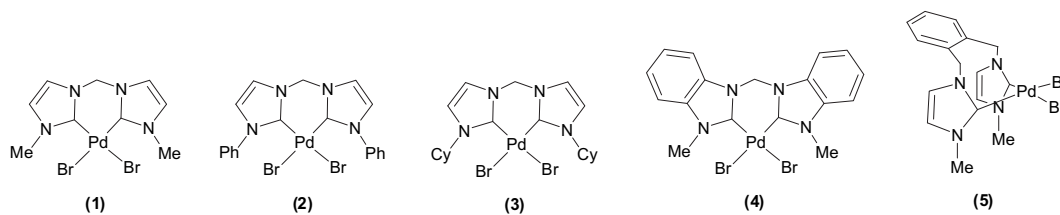


Chart 1.

2. Results and discussion

2.1. Electrochemical investigations

The electrochemical behaviour of Pd(II)-dicarbene complexes **1**–**5** has been analysed by cyclic voltammetry under different experimental conditions in DMSO. The complexes exhibit quite similar voltammetric features, which will be illustrated in details in the case of complex **1**, chosen as an example.

The complex displays a well defined reduction peak, followed by a second one of much lower current intensity. No anodic peaks associated with these reduction processes have been observed in the reverse positive-going scan even at high scan rates (Fig. 1).

Considering the well known redox properties of palladium, the observed cathodic peaks can be attributed to the reduction of Pd(II) to Pd(0) [7a].

The absence of anodic partners of the reduction peaks is indicative of irreversible processes, which may be related to slow electron transfer to Pd(II) (electrochemical irreversibility) or to instability of the reduced species of Pd(0) (chemical irreversibility) or to both of them.

An interesting aspect about the voltammetric behaviour of the complex is the presence of two peaks, though of dissimilar height. This indicates the presence of different species in solution, most likely due to the substitution of the halide anions bound to the metal with coordinating solvent molecules. Therefore, firstly it was deemed necessary to precisely assign the reduction peaks, considering all the possible complexation equilibria involving Pd(II) species.

The complex is introduced into solution as [Pd(dicarbene)Br₂], but, upon dissolution in DMSO, it may lose in principle one or both

bromide ions *via* substitution by solvent molecules. As a matter of fact we have found that only one bromide ligand is substituted by DMSO in the presence of a strong electrolyte such as Bu₄NClO₄ (Scheme 1).

The presence of species **1** and **1a** is in accordance with the effect of the scan rate, ν , on the voltammetric response of complex **1**. Note that although these two species are related by a reversible chemical reaction, they should give rise to two distinct reduction peaks as long as they are present in the vicinity of the electrode in the time-scale of the experiment. However, the current intensities of their reduction peaks may be affected by the time-scale of the CV experiment. Indeed, as ν is increased, the normalized current $I/\nu^{1/2}$ of the second peak increases at the expense of the first and this is a safe evidence of the existence of at least two palladium(II) species in equilibrium (Fig. 1).

Clearly the process underlying the first peak is the reduction of a species whose actual concentration changes with scan rate: being this species involved in a reversible chemical reaction, at low scan rates the experiment lasts long enough to allow the chemical reaction to regenerate continuously the electroactive species, which continues to participate in the reduction reaction. At higher scan rates the time-scale of the experiment becomes shorter and the effect of the chemical equilibration is increasingly lowered. Therefore, the current at low ν values corresponds to an apparent substrate concentration near the electrode, which is higher than the initial equilibrium concentration in the bulk solution. The results described so far are compatible with the occurrence of the first equilibrium shown in Scheme 1, the observed two peaks being assigned to **1** and **1a**.

A further evidence of the existence of an equilibrium involving different Pd(II) species is provided by an experiment performed in the presence of excess bromide ions in order to create conditions favouring the predominance of [Pd(dicarbene)Br₂]. The effect of added tetraethylammonium bromide (TEABr) (up to [Br⁻]/[Pd^{II}] = 50) on the voltammetric pattern of **1** is illustrated in Fig. 2. As the concentration of Br⁻ is increased, the second reduction peak increases at the expense of the first. When 50-fold TEABr is added, the first peak almost disappears (only a shoulder can be observed), while the second develops to a well-defined peak, with a peak potential, E_p , of -2.0 V vs Fc^{+/0} at $\nu = 0.1$ V s⁻¹. This peak is still attributed to **1**, the difference between the E_p values observed in the two experiments (-2.0 V at $\nu = 0.1$ V s⁻¹ vs -2.4 V at $\nu = 20$ V s⁻¹) being simply due to the different scan rates used; in fact identical E_p values are obtained for **1** in the absence and in the presence of excess Br⁻, provided that the CV experiments are run with the same time-scale and the scan rate is high enough to avoid interference from the dynamic equilibrium between **1** and **1a**. It is quite reasonable to assume that, in the presence of a large excess of Br⁻, the complex with the two bromide ligands is the predominant species in solution. It is therefore possible to assign the second reduction peak of **1** to the dibromo complex, [Pd(carbene)Br₂].

To confirm the existence of an equilibrium between **1** and **1a**, the voltammetric investigation on complex **1** in DMSO has been extended to positive potentials, where oxidation of bromide ions

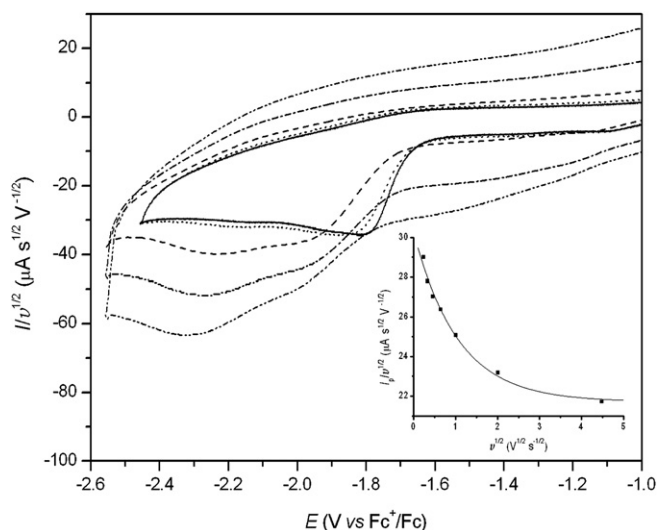
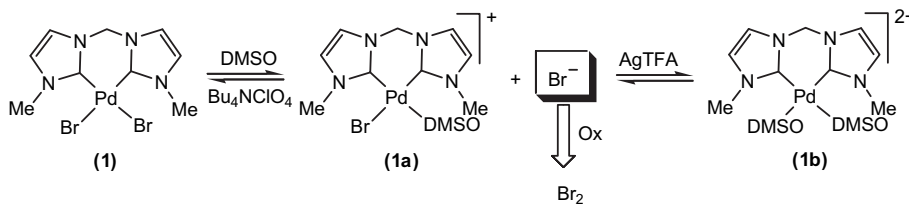


Fig. 1. Cyclic voltammetry of 1.51 mM **1** in DMSO + 0.1 M Bu₄NClO₄ recorded at different scan rates ν : 0.1 V s⁻¹ (—), 0.2 V s⁻¹ (·····), 2 V s⁻¹ (— —), 6 V s⁻¹ (— · —), 20 V s⁻¹ (— · — · —); in the insert, dependence of the normalized peak current of the first peak on the scan rate.



Scheme 1. Species formed dissolving complex **1** in DMSO containing 0.1 M Bu_4NClO_4 and schematic representation of the oxidation of bromide ions stemming from the dissociation of **1** into **1a** and Br^- .

can be detected. It is worth noting that, just like the reduction of **1a**, the electrochemical oxidation of Br^- may shift the equilibrium between species **1** and **1a** towards the release of further bromide anions (Scheme 1).

Therefore the voltammetric response for the oxidation of Br^- will depend not only on its equilibrium concentration at the beginning of the experiment, but also on the rate of conversion of **1** into **1a**. In fact, we have observed that by increasing the scan rate the normalized peak current, $I_{\text{pa}}/v^{1/2}$, for the oxidation peak of the bromide ions decreases and approaches a limiting value, which corresponds to the “real” Br^- equilibrium concentration (more details in the Supporting Information).

It may be concluded that, at low $[\text{Br}^-]/[\text{Pd(II)}]$ ratios or in the absence of added $[\text{Br}^-]$, **1** partially dissociates to give mainly **1a**. Moreover, upon addition of silver trifluoroacetate (AgTFA) 2/1 to complex **1** both of its original peaks disappear, while a new peak appears at -1.72 V vs Fc^+/Fc . Addition of Ag^+ to a solution of **1** causes precipitation of AgBr , drastically modifying the equilibrium depicted in Scheme 1. The coordination sites left vacant by the precipitating bromide ions may be occupied by solvent molecules, DMSO, by TFA^- , or even by the ClO_4^- ions of the background electrolyte. To exclude the possibility that the TFA^- or ClO_4^- anions can efficiently compete with the DMSO solvent as ligands towards the Pd(II) centre, we have carried out two additional experiments with silver salts. In the first one AgBF_4 has replaced AgTFA , so that precipitation of AgBr involves introduction in solution of a very poor coordinating ion such as BF_4^- . The second experiment was performed with Bu_4NBF_4 as base electrolyte and AgBF_4 as the silver salt, to avoid the presence in solution also of ClO_4^- . As shown

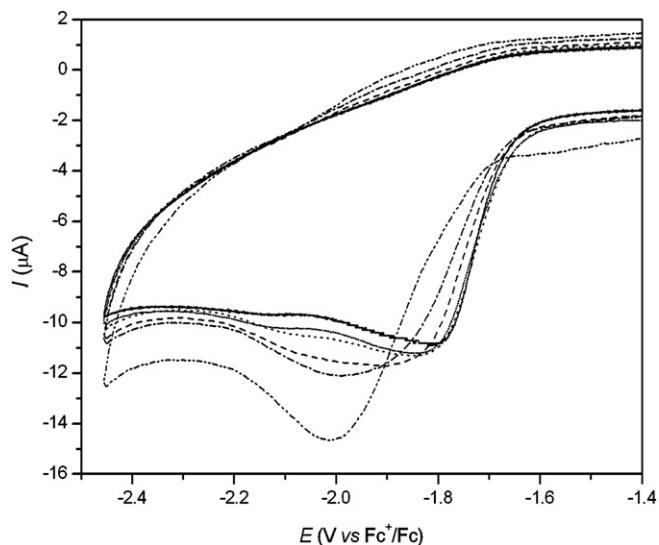


Fig. 2. Cyclic voltammetry of 1.51 mM **1** in DMSO + 0.1 M Bu_4NClO_4 , recorded at 0.1 V s^{-1} in the presence of TEABr; the numbers stand for $[\text{Br}^-]/[\text{Pd(II)}]$: 0 (—), 1 (⋯), 2 (— · — ·), 5 (---), 10 (— — —), 50 (— · — ·).

in Fig. 3, both these tests give virtually the same results as that of the experiment conducted in DMSO + 0.1 M Bu_4NClO_4 , using AgTFA to precipitate silver bromide. In all experiments, elimination of Br^- ions results in the disappearance of the original reduction peaks of **1** and the appearance of a new reduction peak at more positive potentials ($E_p = -1.70 \pm 0.01$ V vs Fc^+/Fc at $v = 0.1 \text{ V s}^{-1}$). This result points out that the same complex is formed both in the absence and presence of TFA^- , ClO_4^- , or BF_4^- . It is reasonable that, in the presence of a non-coordinating anion such as BF_4^- , precipitation of AgBr affords the bis-solvento cation $[\text{Pd}(\text{dicarbene})(\text{DMSO})_2]^{2+}$ **1b** to which the new reduction peak can be attributed. Moreover, the newly formed complex is more easily reducible than **1** and **1a**, indicating a decrease of the electron density on the Pd(II) ion. The first peak in the cyclic voltammetry of **1** in the absence of added silver salt can be therefore attributed to the reduction of the monohalide complex **1a**.

In order to confirm these conclusions, we have recorded the cyclic voltammetry of a DMSO solution of an authentic sample of the complex 1,1'-dimethyl-3,3'-methylene-dibenzimidazolin-2,2'-ylidene)palladium(II) bis(trifluoroacetate), the trifluoroacetate analogue of complex **4** [2a], which shows a single cathodic peak at about -1.5 V, corresponding to the reduction of the bis-solvento cation **4b**. The same result has been obtained by CV analysis of **4** in the presence of 2-fold AgBF_4 .

In conclusion, the main voltammetric peak observed in the CV of complex **1** at low scan rates (for example at 0.1 V s^{-1}) is related to the mixed species $[\text{Pd}(\text{dicarbene})(\text{Br})(\text{DMSO})]^+$ **1a**, since under

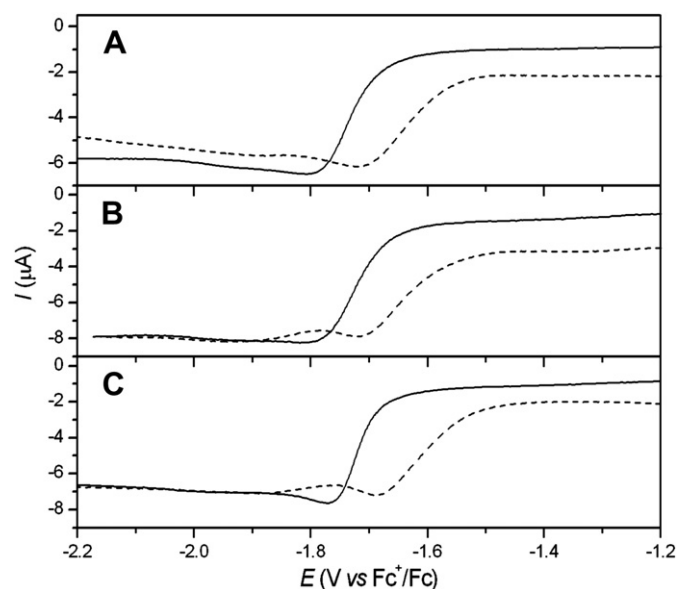


Fig. 3. Cyclic voltammetry of **1** recorded at $v = 0.1 \text{ V s}^{-1}$ in the absence (full lines) and presence (dashed lines) of a 2-fold excess of a silver salt, AgX : (A) solvent = DMSO + 0.1 M Bu_4NClO_4 , X = TFA^- ; (B) solvent = DMSO + 0.1 M Bu_4NClO_4 , X = BF_4^- ; (C) solvent = DMSO + 0.1 M Bu_4NBF_4 , X = BF_4^- .

these conditions just one halide ligand is removed from the Pd(II) complex. Addition of a large excess of Br⁻ moves the equilibrium towards the starting [Pd(dicarbene)Br₂] **1** and the main reduction peak observed is related to this complex. When, instead, soluble silver salts are added to the solution, the prevailing species becomes the *bis*-solvento complex [Pd(dicarbene)(DMSO)₂]²⁺ **1b** and its reduction gives a well defined peak at potentials more positive than that of **1a** or **1**.

After this preliminary identification of the equilibria in solution for **1**, the study was extended to the remaining complexes **2–5**, which display very similar voltammetric features resembling much that described for **1**.

The voltammetric response of each complex was examined at different scan rates from 0.05 to 20 V s⁻¹. As *v* is increased, the main cathodic peak decreases in height, while a new peak appears at more negative potentials. Both peaks are irreversible even at high scan rates and shift to more negative potentials with increasing *v*. As mentioned earlier, the absence of anodic peaks, attributable to the oxidation of the electrogenerated Pd(0) species, may be due to instability of the latter or to slow electron transfer, ET, to Pd(II). In either case, an increase of *v* will cause a cathodic shift of the peak, as it is actually observed. However, if the overall process is kinetically controlled by the ET (irreversible ET), *E_p* is expected to vary linearly with log*v* with a slope $\partial E_p/\partial \log v$ significantly smaller than -30 mV [10].

This analysis has been carried out for all complexes as such and in the presence of TEABr or AgTFA, that is, under conditions favouring the formation of [Pd(dicarbene)(Br)DMSO]⁺ **na**, [Pd(dicarbene)Br₂] **n** or Pd(dicarbene)(DMSO)₂²⁺ **nb**, respectively. Table 1 reports the peak potentials recorded at 0.1 V s⁻¹ together with the slopes of the *E_p* vs log*v* plots.

The values of the slope $\partial E_p/\partial \log v$ are much more negative than -30 mV for all of the complexes **n**, **na** and **nb** (in the range -53 to -132 mV), indicating reduction processes under kinetic control of

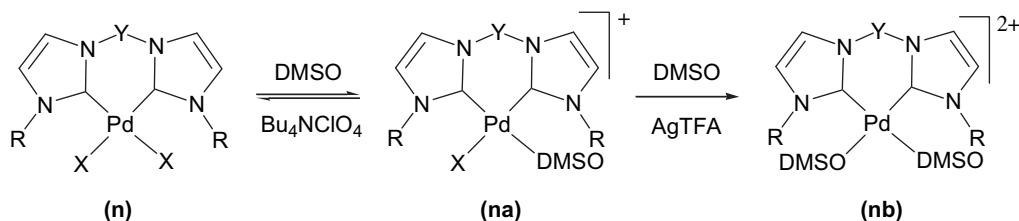
the ET. Moreover, the derived values of the transfer coefficients α (last column of the tables) differ from the ideal value of 0.5, typical of a very fast and reversible process; this indicates a sluggish electron transfer process, as expected for a transformation involving considerable structural changes accompanying the passage, upon ET, from a square planar Pd(II) to a tetrahedral Pd(0). The behaviour of complex **3a** is different from those of the other complexes of the series. It shows a $\partial E_p/\partial \log v$ slope of -31 mV, which is typical of a relatively fast ET followed by an irreversible chemical reaction. In this case, the overall reduction process is kinetically controlled by the decomposition of the electrogenerated Pd(0) complex.

Unfortunately, the standard reduction potentials of these Pd(II) complexes cannot be measured because of the irreversibility of the ET. However, considering that the peak potentials are related to the standard reduction potentials, *E_p* values measured at a fixed scan rate (say 0.1 V s⁻¹) may be used in place of *E⁰* for a comparative analysis of the redox properties of the complexes. It should be stressed that *E_p* contains kinetic effects also, which for simplicity have been taken to be constant, assuming that the standard heterogeneous ET rate constant does not significantly vary in each series of Pd complexes.

Unlike the other investigated Pd(II) complexes, **5** was found to be quite resistant to the complete release of bromide ions. In fact, addition of a 2-fold excess of AgTFA to **5** causes only a partial conversion of **5a** into the *bis*-solvento complex **5b** and therefore the cyclic voltammetry shows two partially overlapping peaks related to these species. The presence of a remarkable amount of **5a** even after addition of AgTFA makes quite difficult to obtain reliable electrochemical parameters for **5b**. Nevertheless, while precise analysis of the dependence of *E_p* on log*v* could not be achieved, the voltammetric response at 0.1 V s⁻¹ allowed a rough measure of *E_p* to be made.

Comparing the peak potentials obtained at 0.1 V s⁻¹ for the same series of different complexes, it is evident that the NHC ligand

Table 1
Voltammetric data for the reduction of Pd(II) complexes in DMSO + 0.1 M Bu₄NClO₄.



| Complex | c [mM] | <i>E_{pc}</i> ^a [V vs Fc ⁺ /Fc] | $\partial E_{pc}/\partial \log v$ [mV] | α^b |
|-----------------------|--------|---|--|------------|
| 1^c | 0.86 | -2.00 | -82 | 0.36 |
| 2^c | 0.89 | -2.11 | -90 | 0.33 |
| 3^c | 0.94 | -2.14 | -79 | 0.37 |
| 4^c | 0.55 | -2.02 | -61 | 0.48 |
| 5^c | 0.99 | -2.38 | -66 | 0.45 |
| 1a | 0.86 | -1.81 | -132 | 0.22 |
| 2a | 0.84 | -1.88 | -99 | 0.30 |
| 3a | 0.94 | -2.00 | -31 | - |
| 4a | 1.51 | -1.82 | -123 | 0.24 |
| 5a | 0.87 | -2.00 | -80 | 0.37 |
| 1b^d | 0.86 | -1.72 | -65 | 0.46 |
| 2b^d | 0.84 | -1.69 | -60 | 0.50 |
| 3b^d | 0.76 | -1.83 | -53 | 0.56 |
| 4b^d | 1.51 | -1.59 | -70 | 0.42 |
| 5b^d | 1.51 | -1.77 | - | - |

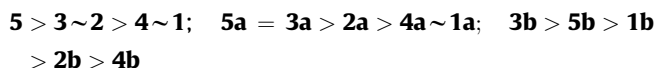
^a Cathodic peak potential, *E_{pc}*, measured at *v* = 0.1 V s⁻¹.

^b $\alpha = -29.6/(\partial E_{pc}/\partial \log v)$.

^c Prepared in situ by addition of a 50-fold excess of TEABr to a solution of [Pd(dicarbene)Br₂].

^d Prepared in situ by addition of a 2-fold excess of AgTFA to a solution of [Pd(dicarbene)Br₂].

significantly affects the electron density at the metal centre. If it is assumed that the reduction potential is related to the charge density on Pd in the sense that the greater the electron density on the metal, the lower the reduction potential, the electron density present on palladium(II) decreases in the following order:



The electron density on Pd(II) is the lowest for species derived from complexes **1** and **4**, since they show the least negative reduction potentials. In contrast, species derived from complex **5** have the most negative potentials and, hence, the highest electron density on the metal.

In general, the reduction potentials of the *bis*-solvento complexes **nb** are less negative than those of the corresponding monohalide complexes **na**, since dicationic species $[\text{Pd}(\text{dicarbene})(\text{DMSO})_2]^{2+}$ are more easily reduced than the monocationic species $[\text{Pd}(\text{dicarbene})(\text{Br})(\text{DMSO})]^+$.

2.2. NMR characterisation

The different electronic properties at the metal centre in complexes **1–5** can be evaluated also from their ^{13}C NMR spectra. Several research groups have in fact demonstrated that the ^{13}C chemical shift of the carbene carbon atom in N-heterocyclic monocarbene complexes moves upfield as the metal centre is made more electron-poor by ligand exchange [11]. This observation also forms the basis of a method for the evaluation of the electron-donating properties of ligands L in complexes of the type *trans*- $[\text{PdBr}_2(\text{}^i\text{Pr}_2\text{-bimy})\text{L}]$ ($\text{}^i\text{Pr}_2\text{-bimy}$ = 1,3-diisopropylbenzimidazolin-2-ylidene), which has recently been proposed by Huynh et al. [9].

We have confirmed these upfield shifts by comparing the ^{13}C NMR spectrum of complex **1** with that of the *bis*-solvento complex **1b** obtained in situ by addition of a 2-fold excess of AgBF_4 . Substitution of the coordinated bromides by DMSO causes a higher shielding of the NMR carbene carbon signals (145.9 ppm (**1b**) vs 168.5 ppm (**1**)).

We have also registered the spectra of complexes **1, 3–5** in DMSO-d_6 and both ^1H and ^{13}C NMR spectra present a single set of signals, indicating a highly symmetric structure. In accordance with the literature data [11] the only observed species are the dihalide complexes **n** and there is no evidence of bromide dissociation from the complexes in the absence of added strong electrolytes. Since the complexes differ only for the employed dicarbene ligand, the resulting differences in electronic properties at the palladium centre are dependent on the electron-donating properties of the coordinated dicarbene. Consequently, we can suppose a correlation between the electron density at the metal and at the carbene carbon atom, expressed by its ^{13}C chemical shift.

The chemical shift values for the various complexes were plotted against their respective E_{pc} values in Fig. 4. A linear correlation is evident for data regarding complexes **1, 3** and **4**, whereas complex **5** falls off-correlation. We have interpreted this discrepancy by considering that, compared to complexes **1–4**, **5** has a different bridging group between the two carbenes. This leads to the two carbene groups having widely different orientations with respect to the plane defined by the Pd centre and by the two bromide ligands. In particular, the dihedral angles between the Br–Pd–Br plane and the carbene rings are 85.1° and 79.2° in complex **5** [12], whereas they are about $50\text{--}55^\circ$ for all known complexes with a methylene spacer, irrespective of the nature of the heterocycle, of the wingtip substituents and of the

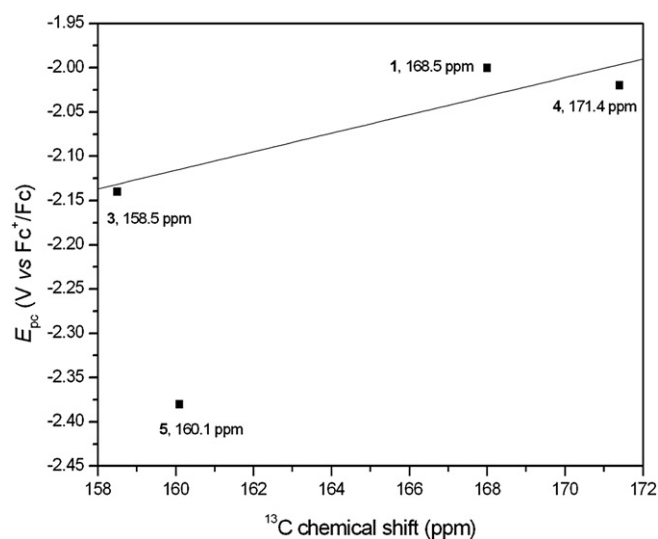


Fig. 4. Correlation of the reduction peak potentials of $[\text{Pd}(\text{dicarbene})\text{Br}_2]$, measured at $v = 0.1 \text{ V s}^{-1}$ in $\text{DMSO} + 0.1 \text{ M Bu}_4\text{NClO}_4$, with the ^{13}C chemical shift of the carbene carbon.

anionic ligands at palladium [13]. Furthermore, the C–Pd–C angle in complex **5** is 89.7° , whereas the constraints imposed by the methylene spacer reduce it to $83\text{--}84^\circ$ for all other complexes. Thus, it can be expected that the different position and orientation of the carbene rings will affect the electron-donating capabilities of the ligand resulting in different electronic properties at the palladium centre as compared to those of the other complexes. On the contrary, for complexes with the same bridging group the correlation between the electron density at the metal and at the carbene carbon atom is evident, showing the expected dependence on the nature of the wingtip substituent: for example, the electron donation of a cyclohexyl substituent to the imidazole ring is greater than that of a methyl group, as indicated by the higher shielding of the coordinated carbene carbon (158.5 ppm (**3**) vs 168.5 ppm (**1**)). Furthermore, use of a benzimidazole moiety (complex **4**) instead of an imidazol-2-ylidene (complex **1**) leads to a lower shielding of the carbene ^{13}C signal (171.4 ppm (**4**) vs 168.5 ppm (**1**)), as a consequence of a more extensive electron delocalisation in the condensed aromatic ring.

The whole set of data obtained by ^{13}C NMR demonstrates that the electron density at the carbene carbon increases in the following order: **4** < **1** < **5** < **3**. Most notably, this trend qualitatively reflects to a certain degree the variations of E_{p} registered by cyclic voltammetry in the series of complexes with the same bridging group (i.e. with the same three-dimensional structure), which indicates a balance between the electron density at the palladium centre and at the carbene carbon.

2.3. XPS characterisation

The variation of electron density at the palladium centre as a consequence of the different N-heterocyclic carbene ligands was also investigated by X-ray Photoelectron Spectroscopy (XPS). In particular, the palladium(II)-dicarbene complexes **1, 3** and **4** were analysed.

Fig. 5 shows the detailed XP spectra of Pd 3d, Br 3d and N 1s, whereas the peak positions are summarized in Table 2.

The binding energies of the Pd 3d core level are consistent with the values reported in the literature for palladium(II) compounds [14]. Albrecht et al. observed an important change of

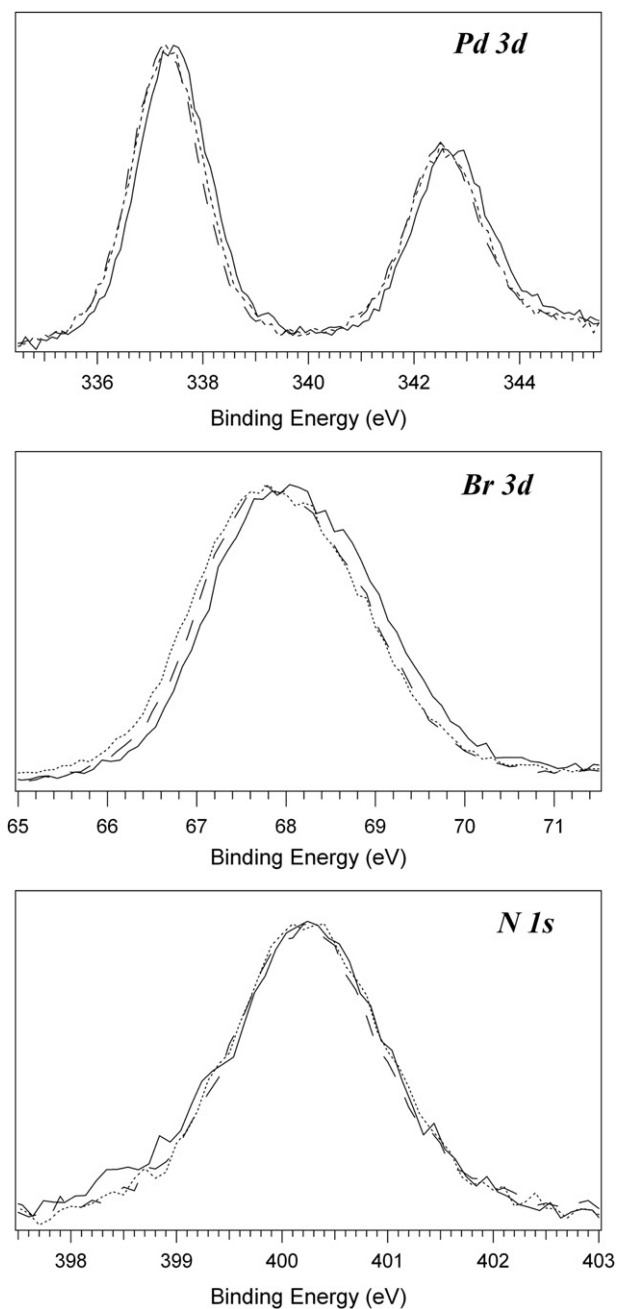


Fig. 5. Pd 3d, Br 3d and N 1s XP spectra of **1** (—), **3** (.....) and **4** (---). (The spectra were normalized with respect to their maximum and minimum values).

the electron density at the palladium centre comparing C2- and C4-bound carbene complexes [8]. It is generally accepted, in fact, that abnormal carbenes (C4 bound) are much stronger electron donor ligands than their C2 bound analogues [15]. Herein, as

Table 2
XPS peak positions (Binding Energy, eV) obtained for complexes **1**, **3** and **4**.

| Complex | Pd 3d | Br 3d | N 1s |
|----------|-------|-------|-------|
| 1 | 337.3 | 67.7 | 400.2 |
| | 342.5 | | |
| 3 | 337.3 | 67.7 | 400.2 |
| | 342.5 | | |
| 4 | 337.4 | 67.8 | 400.2 |
| | 342.7 | | |

a general consideration, the comparison of the three C2-bound dicarbene complexes did not reveal significant changes in the binding energy of Pd 3d as a function of the ligand structure. It is interesting to note, however, that the binding energy of Pd 3d in complexes **1** and **3** is slightly lower than that of palladium in complex **4**. The same trend is observed for the Br 3d XP peak. This could suggest a slightly higher electron density at the palladium centre in complexes **1** and **3** with respect to **4**, which is in good agreement with the cyclic voltammetry and ^{13}C NMR results presented above. By contrast, the binding energies measured for the N 1s core level of the three complexes have identical values, which are consistent with those reported in the literature for nitrogen bound to carbon [14].

Thus, considering the whole set of XPS data shown above, it is fairly difficult to determine the electron donating abilities of a C2-bound carbene using XPS techniques because the differences in the Pd 3d binding energies for complexes **1**, **3** and **4** are too small and close to the precision of the measurement (± 0.1 eV). For this reason evaluation of the electron-donating properties of a carbene ligand via cyclic voltammetry or ^{13}C NMR spectroscopy seems at this stage a more useful approach.

3. Conclusions

In conclusion, we have investigated the electronic properties of a series of N-heterocyclic dicarbene palladium(II) complexes via three different techniques: cyclic voltammetry, ^{13}C NMR spectroscopy and XPS. The technique yielding the most reliable results appears to be cyclic voltammetry, which gives a direct measure of the electron density on the palladium centre. ^{13}C NMR can be proficiently employed only when comparing complexes with the same three-dimensional structure and with the same ligand set apart from the dicarbene ligand itself. Finally, XPS appears to be not enough sensitive for accurately monitoring the change in the electron density of the palladium centre in C2-bound carbene complexes.

The data obtained with the three techniques are consistent and confirm that the electronic properties of the palladium(II) centre depend on the type of dicarbene ligand and, in particular, on the substituents at the nitrogen atom in 3 position, the bridging group between the carbene units and the type of heterocyclic ring. This supports the possibility of finely tuning the electron density at the metal centre by tailoring the dicarbene ligand.

On the other hand, the interesting information on the electronic properties of dicarbene palladium(II) complexes obtained in this study makes it apparent that the electron density at the metal centre is not the exclusive factor determining the catalytic activity of these complexes in the hydroarylation reaction between pentamethylbenzene and ethyl propiolate [2]. In this reaction the observed reactivity order was $\mathbf{2} > \mathbf{4} > \mathbf{1} > \mathbf{5}$, which only partially mirrors the trend in electronic density at the palladium centre determined in this study: although the low efficiency showed by **5** in a reaction involving electron-poor Pd species is in accordance with the higher electron density at the metal centre, **2** was found to be more active and **1** less active than expected, if considering only the electronic properties of the ligand. The most obvious explanation is that the catalytic activity observed in this reaction is influenced also by steric factors; this explanation is further supported by the finding that when a more sterically encumbered reagent (ethyl phenylpropiolate) is used, the reactivity order is completely reversed [2a]. These results highlight once more the importance of a delicate balance between the steric and electronic properties of the metal centre and of the reagents in determining the overall efficiency of the catalytic system.

4. Experimental

4.1. Reagents and apparatus

The reagents were purchased from Aldrich as high purity products and generally used as received. All solvents were used as received as technical grade solvents. Complexes **1** [13b,16], **2** [17], **3** [18], **4** [2c], 1,1'-dimethyl-3,3'-methylenedibenzimidazolin-2,2'-ylidene)palladium(II) bis(trifluoroacetate) [2a] and **5** [12,19] were synthesised according to literature procedures. The solution ^1H - and $^{13}\text{C}\{^1\text{H}\}$ -NMR spectra were recorded on a Bruker Avance 300 (300.1 MHz for ^1H and 75.5 MHz for ^{13}C); chemical shifts (δ) are reported in units of ppm relative to the residual solvent signals, using tetramethylsilane as internal standard. XPS spectra were recorded using a Perkin–Elmer PHI 5600 ci spectrometer with a standard Al-K α source (1486.6 eV) working at 300 W. The working pressure was less than 1×10^{-8} Pa. The spectrometer was calibrated by assuming the binding energy (BE) of the Au 4f $_{7/2}$ line to lie at 84.0 eV with respect to the Fermi level. Extended spectra (survey) were collected in the range 0–1350 eV (187.85 eV pass energy, 0.5 eV step, 0.025 s step $^{-1}$). Detailed spectra were recorded for the following regions: Pd 3d, Br 3d, N 1s and C 1s (11.75 eV pass energy, 0.1 eV step, 0.2 s step $^{-1}$). The standard deviation in the BE values of the XPS line is 0.10 eV. To take into consideration charging problems the C 1s peak at 285.0 eV was considered and the BE differences were evaluated. The samples for the XPS analysis were processed as a pellet by pressing the powder at ca. 7×10^6 Pa for 10 min; the pellet was then evacuated for 12 h at ca. 1×10^{-3} Pa before measurement.

4.2. Electrochemical measurements

Electrochemical measurements were performed on a computer-controlled Autolab PGSTAT30 potentiostat (Eco-Chimie, Utrecht, Netherlands). All experiments were carried out at 25 °C in a three-electrode cell system using glassy carbon (GC) as a working electrode. The counter-electrode and the reference electrode were a Pt ring and Ag/Ag $^+$ /I $^-$, respectively. All potentials reported in the paper are quoted vs the ferricinium/ferrocene redox couple, which was used as an internal reference system.

The GC electrode was a 3-mm diameter disc embedded in glass, which was fabricated from a GC rod (Tokai, GC-20) and polished to a mirror finish with silicon carbide papers of decreasing grain size (Struers, grit: 500, 1000, 2400 and 4000) followed by diamond paste (3-, 1- and 0.25- μm particle size). Before every experiment it was refreshed by polishing with a 0.25- μm diamond paste followed by ultrasonic rinsing in ethanol for about 5 min.

Acknowledgements

Financial support from the University of Padova (PRAT2008-CPDA085452) is gratefully acknowledged.

Appendix. Supplementary material

Supplementary data associated with this article can be found in the online version at doi:10.1016/j.jorganchem.2010.06.019.

References

- [1] (a) H. Clavier, S.P. Nolan, *Chem. Commun.* 46 (2010) 841; (b) L. Cavallo, A. Correa, C. Costabile, H. Jacobsen, *J. Organomet. Chem.* 690 (2005) 5407; (c) A. Poater, B. Cosenza, A. Correa, S. Giudice, F. Ragone, V. Scarano, L. Cavallo, *Eur. J. Inorg. Chem.* (2009) 1759; (d) D.G. Gusev, *Organometallics* 28 (2009) 6458; (e) H. Clavier, A. Correa, L. Cavallo, E.C. Escudero-Adan, J. Benet-Buchholz, A.M.Z. Slawin, S.P. Nolan, *Eur. J. Inorg. Chem.* (2009) 1767; (f) S. Würtz, F. Glorius, *Acc. Chem. Res.* 41 (2008) 1523.
- [2] (a) A. Biffis, L. Gazzola, P. Gobbo, G. Buscemi, C. Tubaro, M. Basato, *Eur. J. Org. Chem.* (2009) 3189; (b) G. Buscemi, A. Biffis, C. Tubaro, M. Basato, *Catal. Today* 140 (2009) 84; (c) A. Biffis, C. Tubaro, G. Buscemi, M. Basato, *Adv. Synth. Catal.* 350 (2008) 189.
- [3] (a) C. Jia, D. Piao, J. Oyamada, W. Lu, T. Kitamura, Y. Fujiwara, *Science* 287 (2000) 1992; (b) C. Jia, W. Lu, J. Oyamada, T. Kitamura, K. Matsuda, M. Irie, Y. Fujiwara, *J. Am. Chem. Soc.* 122 (2000) 7252; (c) C. Jia, T. Kitamura, Y. Fujiwara, *Acc. Chem. Res.* 34 (2001) 633.
- [4] (a) J.A. Tunge, L.N. Foresee, *Organometallics* 24 (2005) 6440; (b) E. Soriano, J. Marco-Contelles, *Organometallics* 25 (2006) 4542.
- [5] (a) W.A. Herrmann, J. Schütz, G.D. Frey, E. Herdtweck, *Organometallics* 25 (2006) 2437; (b) R.A. Kelly III, H. Clavier, S. Giudice, N.M. Scott, E.D. Stevens, J. Bordner, I. Samardjiev, C.D. Hoff, L. Cavallo, S.P. Nolan, *Organometallics* 27 (2008) 202; (c) N.M. Scott, H. Clavier, P. Mahjoor, E.D. Stevens, S.P. Nolan, *Organometallics* 27 (2008) 3181; (d) R. Dorta, E.D. Stevens, N.M. Scott, C. Costabile, L. Cavallo, C.D. Hoff, S.P. Nolan, *J. Am. Chem. Soc.* 127 (2005) 2485; (e) M. Poyatos, W. McNamara, C. Incarvito, E. Clot, E. Peris, R.H. Crabtree, *Organometallics* 27 (2008) 2128; (f) R.H. Crabtree, *J. Organomet. Chem.* 690 (2005) 5451; (g) J.R. Miecznikowski, R.H. Crabtree, *Polyhedron* 23 (2004) 2857.
- [6] L. Delaude, S. Delfosse, A. Richel, A. Demonceau, A.F. Noels, *Chem. Commun.* (2003) 1526.
- [7] (a) J. Pytkowicz, S. Roland, P. Mangeney, G. Meyer, A. Jutand, *J. Organomet. Chem.* 678 (2003) 166; (b) F. Demirhan, Ö. Yildirim, B. Cetinkaya, *Transit. Met. Chem.* 28 (2003) 558; (c) L. Meres, G. Labat, A. Neels, A. Ehlers, M. Albrecht, *Organometallics* 25 (2006) 5648; (d) S. Leuthäuser, D. Schwarz, H. Plenio, *Chem. Eur. J.* 13 (2007) 7195.
- [8] (a) M. Heckenroth, E. Kluser, A. Neels, M. Albrecht, *Angew. Chem. Int. Ed.* 46 (2007) 6293; (b) M. Albrecht, *Chem. Commun.* (2008) 3601; (c) M. Heckenroth, A. Neels, M.G. Garnier, P. Aebi, A.W. Ehlers, M. Albrecht, *Chem. Eur. J.* 15 (2009) 9375.
- [9] H.V. Huynh, Y. Han, R. Jothibasu, J.A. Yang, *Organometallics* 28 (2009) 5395.
- [10] A.J. Bard, L.R. Faulkner, *Electrochemical Methods*, second ed. Wiley & Sons, New York, 2001.
- [11] (a) W.A. Herrmann, O. Runte, G. Artus, *J. Organomet. Chem.* 501 (1995) C1; (b) M.V. Baker, P.J. Barnard, S.K. Brayshaw, J.L. Hickey, B.W. Skelton, A.H. White, *Dalton Trans.* (2005) 37; (c) Y. Han, H.V. Huynh, G.K. Tan, *Organometallics* 26 (2007) 6447.
- [12] M.V. Baker, B.W. Skelton, A.H. White, C.C. Williams, *J. Chem. Soc. Dalton Trans.* (2001) 111.
- [13] (a) M.A. Taige, A. Zeller, S. Ahrens, S. Goutal, E. Herdtweck, T. Strassner, *J. Organomet. Chem.* 692 (2007) 1519; (b) E. Herdtweck, M. Muehlhofer, T. Strassner, *Acta Crystallogr. Sect. E: Struct. Rep. Online* (2003) m970; (c) F.E. Hahn, M. Foth, *J. Organomet. Chem.* 585 (1999) 241.
- [14] X-ray Photoelectron Spectroscopy Database (Version 3.5). <http://srdata.nist.gov>.
- [15] A.R. Chianese, A. Kovacevic, B.M. Zeglis, J.W. Faller, R.H. Crabtree, *Organometallics* 23 (2004) 2461.
- [16] M.G. Gardiner, W.A. Herrmann, C.-P. Reisinger, J. Schwarz, M. Spiegler, *J. Organomet. Chem.* 572 (1999) 239.
- [17] W.A. Herrmann, J. Schwarz, M.G. Gardiner, *Organometallics* 18 (1999) 4082.
- [18] K. Okuyama, J. Sugiyama, R. Nagahata, M. Asai, M. Ueda, K. Takeuchi, *J. Mol. Catal. A: Chemical* 203 (2003) 21.
- [19] A.M. Magill, D.S. McGuinness, K.J. Cavell, G.J.P. Britovsek, V.C. Gibson, A.J.P. White, D.J. Williams, A.H. White, B.W. Skelton, *J. Organomet. Chem.* 617–618 (2001) 546.